

## II. Cytotoxic benzophenones from *Garcinia macrophylla* (Clusiaceae)

### 2.1 Introduction

In a continuing search for anticancer compounds as part of an ICBG Program an extract of *Garcinia macrophylla* from Suriname, and its ethyl acetate extract was found to be cytotoxic in the A2780 human ovarian cancer cell line cytotoxicity bioassay. The extract was subjected to fractionation, which resulted in the isolation of three compounds. This is the first reported chemical investigation of *G. macrophylla*.

#### 2.1.1 Chemical Investigation of *Garcinia*

*Garcinia macrophylla* (Figure 2.1)<sup>1</sup> is a tropical tree belonging to the family Clusiaceae. It is a rather large tree, as its name suggests, reaching 30 meters in height. The various members of the genus are widespread in the tropical regions of the world.<sup>2</sup> They are used extensively by indigenous people for treatment of a wide range of diseases, and the fruits are even dried and used as a spice. The juice from the leaves of *G.*

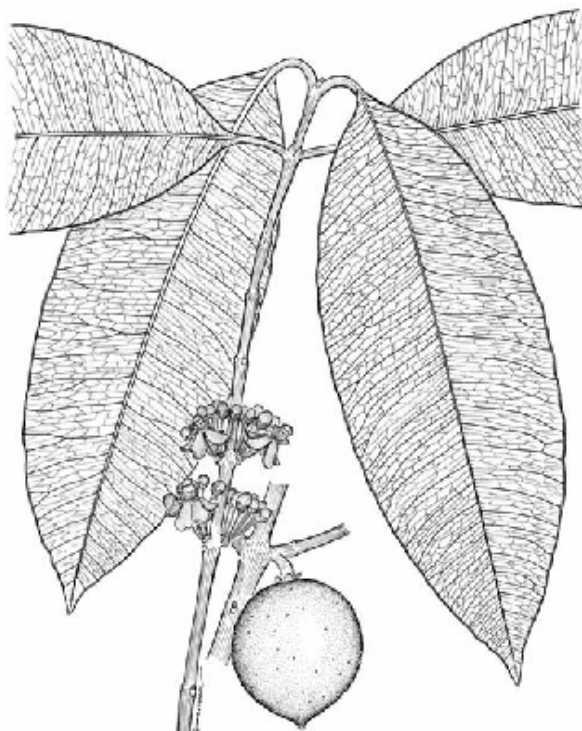


Figure 2.1 *Garcinia macrophylla*.

<sup>1</sup> Missouri Botanical Garden, <http://www.mobot.org>

<sup>2</sup> Thoison, O.; Fahy, J.; Dumontet, V.; Chiaroni, A.; Riche, C.; Tri, M. V.; Sévenet, T. Cytotoxic Prenylxanthenes from *Garcinia bracteata*. *J. Nat. Prod.* **2000**, *63*, 441-446.

*gaudichaudii* is used to rub on cuts and minor wounds.<sup>3</sup> The leaves and seeds of *G. dulcis* have been used to treat lymphatitis, parotitis, struma, and other disease conditions.<sup>4</sup> The fruits of *G. atroviridis* have been used to treat cough, dandruff, earache, stomach pains due to pregnancy, and throat irritation.<sup>5</sup> *G. mangostana* has been used as an anti-inflammatory and antidiarrheal.<sup>6</sup> An Internet search of ‘*Garcinia*’ also reveals its use as an herbal weight loss remedy.

As one would expect from the numerous uses reported, a variety of compounds have been isolated from the genus. The compounds perhaps most associated with the genus are benzophenones (**2.1**, **2.2**) and xanthenes (**2.3**), both of which are typically prenylated. However, depsidones (**2.4**) triterpenes (**2.5**), and flavonoids (**2.6**) have also been reported. The xanthenes have been found to exhibit antifungal,<sup>6</sup> antimicrobial,<sup>7</sup> cytotoxic,<sup>8</sup> antioxidant,<sup>9</sup> antimalarial,<sup>10</sup> and HIV-1 protease inhibitory activity.<sup>11</sup> The

---

<sup>3</sup> Xu, Y. J.; Yip, S. C.; Kosela, S.; Fitri, E.; Hana, M.; Goh, S. H.; Sim, K. Y. Novel Cytotoxic, Polyprenylated Heptacyclic Xanthonoids from Indonesian *Garcinia gaudichaudii* (Guttiferae). *Organic Letters*. **2000**, *2*, 3945-3948.

<sup>4</sup> Iinuma, M.; Ito, T.; Tosa, H.; Tanaka, T. Five New Xanthenes from *Garcinia dulcis*. *J. Nat. Prod.* **1996**, *59*, 472-475.

<sup>5</sup> Permana, D.; Lajis, N. H.; Mackeen, M. M.; Ali, A. M.; Aimi, N.; Kitajima, M.; Takayama, H. Isolation and Bioactivities of Constituents of the Roots of *Garcinia atroviridis*. *J. Nat. Prod.* **2001**, *64*, 976-979.

<sup>6</sup> Gopalakrishnan, G.; Banumathi, B.; Suresh, G. Evaluation of the Antifungal Activity of Natural Xanthenes from *Garcinia mangostana* and Their Synthetic Derivatives. *J. Nat. Prod.* **1997**, *60*, 519-524.

<sup>7</sup> Rukachaisirikul, V.; Kaewnok, W.; Koysomboon, S.; Phongpaichit, S.; Taylor, W. C. Caged-Tetraprenylated Xanthenes from *Garcinia scortechnikii*. *Tetrahedron*. **2000**, *56*, 8539-8543.

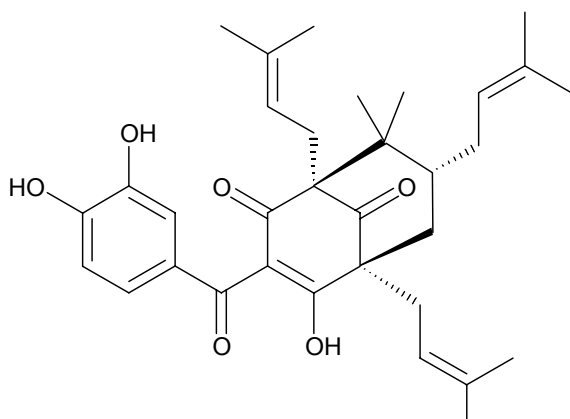
<sup>8</sup> Cao, S. G.; Sng, V. H. L.; Wu, X. H.; Sim, K. Y.; Tan, B. H. K.; Pereira, J. T.; Goh, S. H. Novel Cytotoxic Polyprenylated Xanthonoids from *Garcinia gaudichaudii* (Guttiferae). *Tetrahedron*. **1998**, *54*, 10915-10924.

<sup>9</sup> Minami, H.; Kuwayama, A.; Yoshizawa, T.; Fukuyama, Y. Novel Prenylated Xanthenes with Antioxidant Property from the Wood of *Garcinia subelliptica*. *Chem. Pharm. Bull.* **1996**, *44*, 2103-2106.

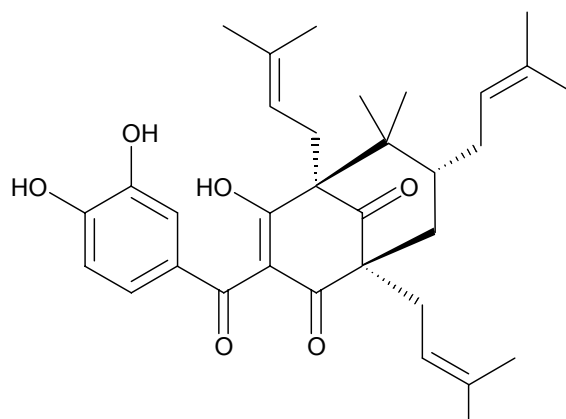
<sup>10</sup> Likhitwitayawuid, K.; Chanmahasathien, W.; Ruangrunsi, N.; Krungkria, J. Xanthenes with Antimalarial Activity from *Garcinia dulcis*. *Planta Med.* **1998**, *64*, 281-282.

<sup>11</sup> Chen, S. X.; Wan, M.; Loh, B. N. Active Constituents Against HIV-1 Protease from *Garcinia mangostana*. *Planta Med.* **1996**, *62*, 381-382.

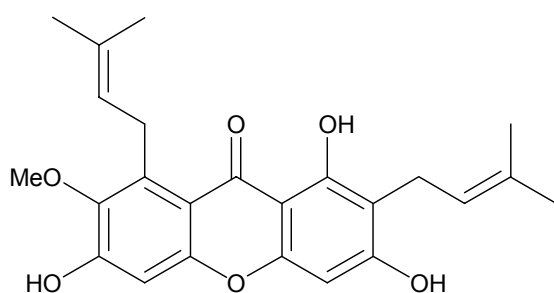
benzophenones have been found to exhibit HIV-inhibitory,<sup>12</sup> antibacterial,<sup>13</sup> antioxidant,<sup>14</sup> and antiulcer activity.<sup>14</sup>



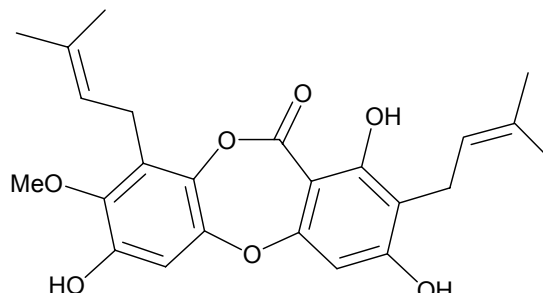
**2.1** Aristophenone A



**2.2** Aristophenone B



**2.3** Mangostin

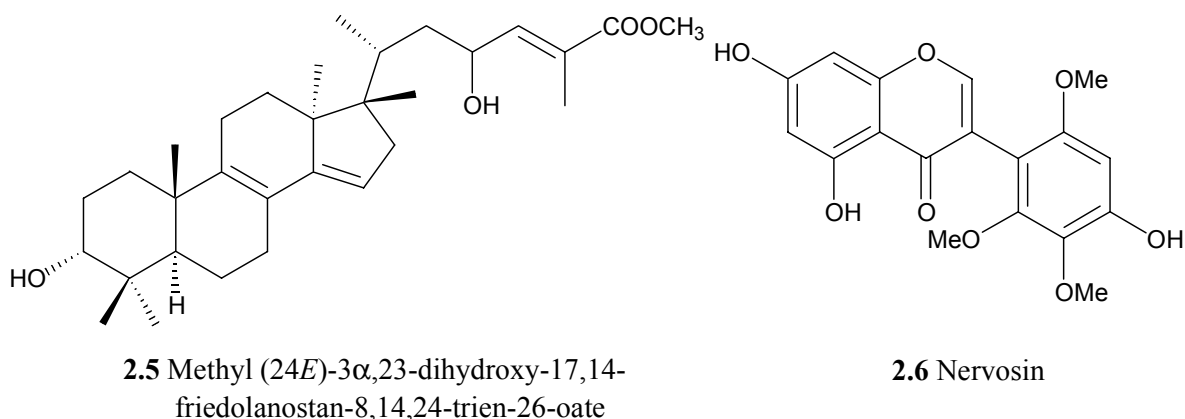


**2.4** Garcinisidone-A

<sup>12</sup> Gustafson, K. R.; Blunt, J. W.; Munro, M. H. G.; Fuller, R. W.; McKee, T. C.; Cardellina, J. H., II; McMahon, J. B.; Cragg, G. M.; Boyd, M. R. The Guttiferones, HIV-Inhibitory Benzophenones from *Symphonia globulifera*, *Garcinia livingstonei*, *Garcinia ovalifolia*, and *Clusia rosea*. *Tetrahedron*. **1992**, *48*, 10093-10102.

<sup>13</sup> Inuma, M.; Tosa, H.; Tanaka, T.; Kanamaru, S.; Asai, F.; Kobayashi, Y.; Miyauchi, K.; Shimano, R. Antibacterial Activity of Some *Garcinia* Benzophenone Derivatives against Methicillin-Resistant *Staphylococcus aureus*. *Biol. Pharm. Bull.* **1996**, *19*, 311-314.

<sup>14</sup> Yamaguchi, F.; Saito, M.; Ariga, T.; Yoshimura, Y.; Nakazawa, H. Free Radical Scavenging Activity and Antiulcer Activity of Garcinol from *Garcinia indica* Fruit Rind. *J. Agric. Food Chem.* **2000**, *48*, 2320-2325.



### 2.1.2 Structural and Medicinal Properties of Benzophenones

The benzophenones that are typically isolated from *Garcinia* are aromatic in only one ring due to prenylation to form a bicyclo[3.3.1]nonane ring system (Figure 2.2). Prenylated benzophenones are thought to be of mixed shikimate and acetate origin. They are found with varying degrees of prenylation, ranging from three to five isoprenyl groups, all contained in the B ring.

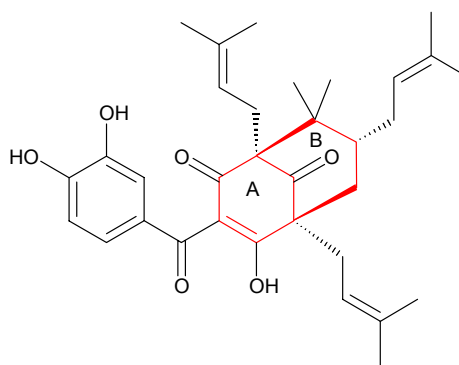


**Figure 2.2** Bicyclo[3.3.1]nonane ring system.

It is interesting to note the presence of an enolized triketone. The presence of the enolized triketone group produces a molecule that is capable of producing a mixture of six tautomers (Figure 2.3). Aristophenone A (**2.1**) and B (**2.2**) provide evidence that at least two tautomers are present. This was confirmed by the presence of a 1:1 ratio of

signals for both  $^{13}\text{C}$  and  $^1\text{H}$  NMR spectra when  $\text{CDCl}_3$  was used as the solvent along with the isolation of the two regio-isomers after acetylation.<sup>15</sup>

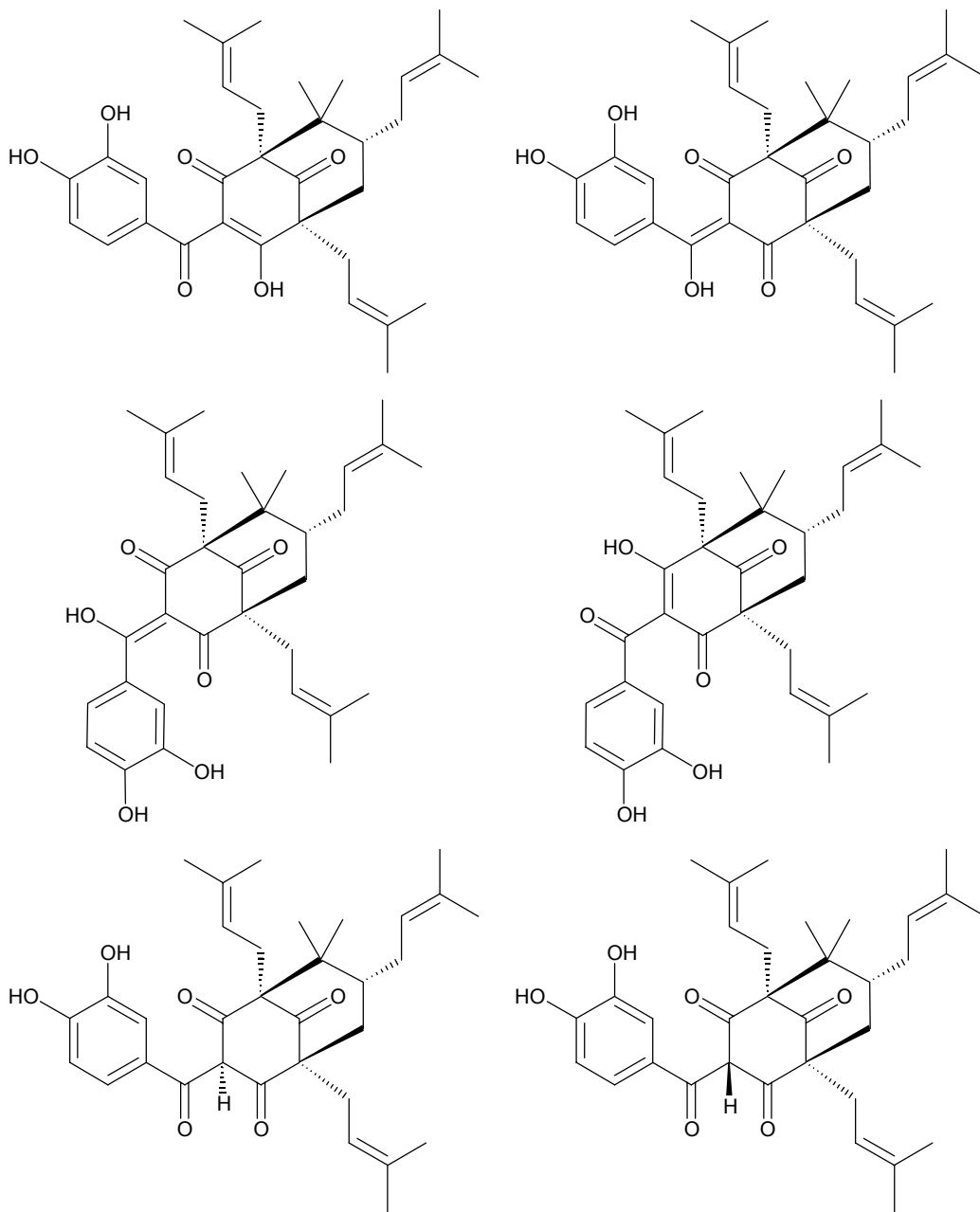


**Figure 2.3** Six possible isomers of aristophenone.

<sup>15</sup> Cuesta-Rubio, O.; Padron, A.; Castro, H. V.; Pizza, C.; Rastrelli, L. Aristophenones A and B. A New Tautomeric Pair of Polyisoprenylated Benzophenones from *Garcinia aristata*. *J. Nat. Prod.* **2001**, *64*, 973-975.

There are currently no examples of prenylated benzophenones being used medicinally in the United States (with the exception of those that may be found in dietary supplements). They are not strongly cytotoxic, which reduces their chances of ever being used medicinally in the United States to treat cancer. However, they do appear to have an interesting mechanism of action. Since the unique mode of action of paclitaxel was discovered there has been a push to find additional tubulin polymerization promoters. It has been reported that at least some benzophenones from *Garcinia* spp. exhibit activity similar to that of paclitaxel, although they are less potent than this compound. As a result there has been at least one publication of structure activity relationship (SAR) studies. None of the derivatives resulted in an increase in tubulin polymerization promoting activity.<sup>16</sup>

## **2.2 Results and Discussion**

### **2.2.1 Isolation of Compounds A, B, and C from *Garcinia macrophylla***

Through continued participation in the ICBG program the crude ethyl acetate extract of *Garcinia macrophylla* was obtained from Suriname. It was found to exhibit weak cytotoxicity (IC<sub>50</sub>=15µg/ml) in the A2780 human ovarian cell line, and thus was selected for detailed investigation.

A portion of the extract (0.5 g) was taken for fractionation (Scheme 2.1). It was first partitioned between 80% aqueous methanol and hexane, and the methanol fraction was then diluted to 50% aqueous methanol and partitioned with dichloromethane. After

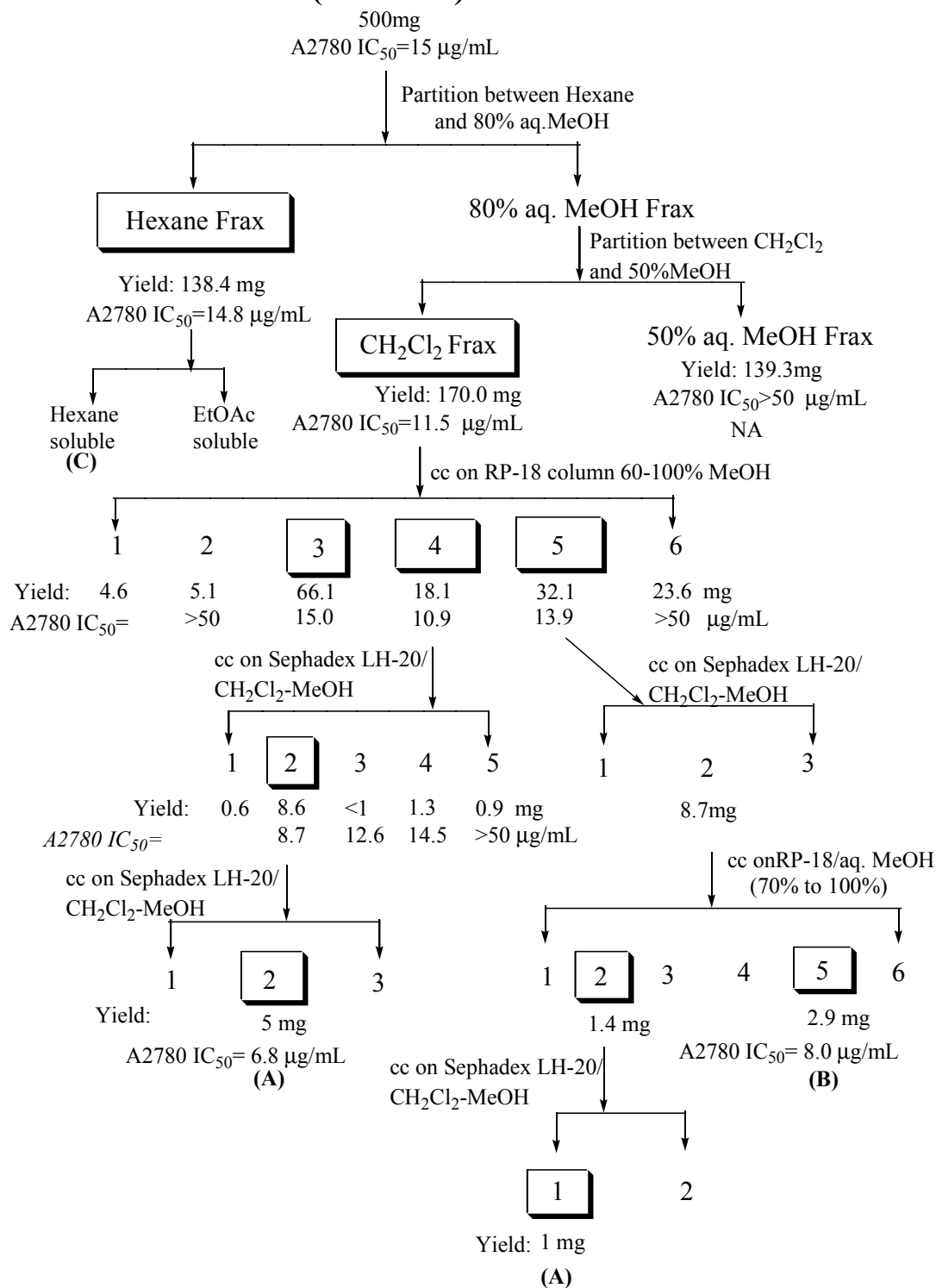
---

<sup>16</sup> Roux, D.; Hadi, H. A.; Thoret, S.; Guénard, D.; Thoison, O.; Païs, M.; Sévenet, T. Structure-Activity Relationship of Polyisoprenyl Benzophenones from *Garcinia pyrifera* on the Tubulin/Microtubule System. *J. Nat. Prod.* **2000**, *63*, 1070-1076.

removal of the solvent by rotary evaporation the hexane and dichloromethane fractions were found to retain the bioactivity while the aqueous methanol fraction was found to be inactive. Because the dichloromethane fraction was more active it was further fractionated with a reversed phase C-18 open column eluted with an aqueous methanol gradient starting at 60% methanol and going to 100% methanol. The two most active fractions (4 and 5) were then separately subjected to column chromatography using Sephadex LH-20 eluted with a gradient starting with dichloromethane and going to 95% dichloromethane / methanol. Fraction 4 was fractionated twice in this manner to give 5 mg of compound **A**. Fraction 5 was further fractionated using RP C-18 eluted with a gradient starting with 70% aqueous methanol to give an additional 1 mg of compound **A** and 2.9 mg of compound **B**. The final purification steps were monitored using RP TLC. RP TLC revealed that the hexane fraction also contained compounds **A** and **B**.

In addition to bioactive compounds **A** and **B** an inactive third compound was obtained from the initial bioactive hexane fraction. This fraction was partitioned into an ethyl acetate soluble fraction and an insoluble fraction. The insoluble fraction was an amorphous white solid, which was recrystallized from dichloromethane and methanol to give colorless needles of **C**.

## *Garcinia macrophylla* (E950358)



**Scheme 2.1** Fractionation tree for *Garcinia macrophylla*.



### 2.2.2 Structural Elucidation of Compound A

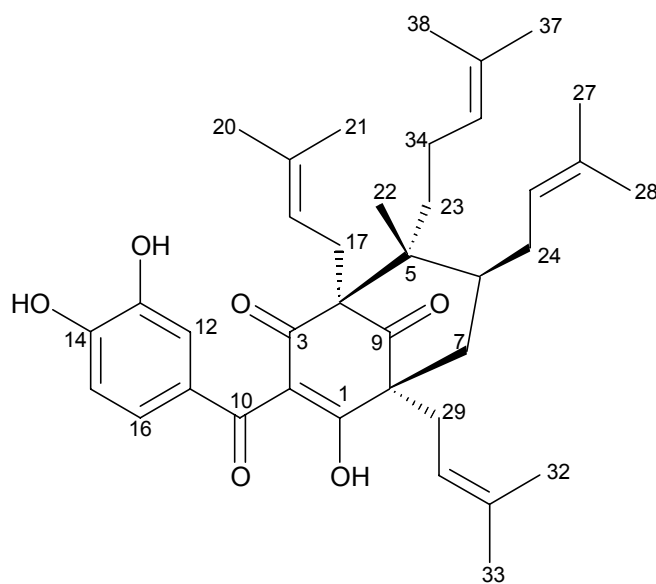
Compound **A** was isolated as a yellow oil. Its negative ion FAB mass spectrum indicated a molecular weight of 602 and a possible molecular formula of  $C_{38}H_{50}O_6$ . Fragment ions at  $m/z$  533, 395, and 326 indicated the loss of four isoprene units. A subsequent search of compounds previously isolated from *Garcinia* species indicated that polyprenylated benzophenones were the most likely class of compounds.

The  $^1H$  NMR spectrum of **A** in  $CDCl_3$  consisted of a multiplicity of peaks, and indicated that, contrary to the TLC data, the sample was still a mixture. However, when the  $^1H$  NMR spectrum was obtained in  $d_4$ -methanol with 0.1% TFA it was greatly simplified. The simplification of the spectrum when  $d_4$ -methanol with 0.1% TFA was used instead of  $CDCl_3$  further indicated that compound **A** was a polyprenylated benzophenone.<sup>12,15</sup> For example the known prenylated benzophenone guttiferone A (**2.7**) gave a complex spectrum in  $CDCl_3$  but was greatly simplified in  $d_4$ -methanol with 0.1% TFA. The  $^1H$  NMR spectrum in  $d_4$ -methanol indicated the presence of one aliphatic  $CH_3$  ( $\delta$  1.25(s)) and eight allylic  $CH_3$ 's ( $\delta$  1.47 (s), 1.59 (s), 1.64 (s), 1.65 (s), 1.67 (s) 9H's, 1.72 (s)). There were three signals for vinylic protons ( $\delta$  4.92 (m), 5.08 (dddd  $J=7.1, 7.1, 1.4, 1.4$ ), 5.19 (ddd  $J=6.6, 6.6, 1.2$ )). An AMX spin system for three aromatic protons was also present ( $\delta$  6.69 (d,  $J=8.5$  Hz), 6.97 (dd,  $J=2.2, 8.5$  Hz), 7.16 (d,  $J=2.2$  Hz)).

The  $^{13}C$  NMR spectrum of **A** in  $CDCl_3$  was similar to the  $^1H$  NMR in that it also appeared to consist of a mixture. The number of signals present was sixty-eight, which is not possible for a molecular weight of 602. The  $^{13}C$  NMR spectrum in  $CDCl_3$  also appeared to contain six signals for saturated quaternary carbons ( $\delta$  50.9, 51.5, 58.8, 63.0, 66.6, 69.6). The  $^{13}C$  NMR and APT spectra in  $d_4$ -methanol with 0.1% TFA were much

clearer. They contained signals for thirty-five carbons, as opposed to the sixty-eight seen in CDCl<sub>3</sub>, further supporting the conclusion that compound **A** exists as a mixture of tautomers. Based on the NMR data, there were eight methyl signals, six saturated methylene signals, one saturated methine signal, one saturated quaternary carbon signal, seven unsaturated methine signals, eight unsaturated quaternary carbon signals, and four carbonyl signals. The methyl signal found at  $\delta$  26.3 was of double intensity, indicating that two methyls were overlapping and thus indicating the presence of nine methyls, as confirmed by the <sup>1</sup>H NMR spectrum. It was possible to detect two additional saturated quaternary carbons using HMBC; the correlations for these carbons were found at  $\delta$  62.1 and 68.8. The absence of those two signals in the <sup>13</sup>C NMR spectrum can be explained by the fact that saturated quaternary carbons typically have long relaxation times and the sample size was limited, leading to the loss of weak signals.

The <sup>1</sup>H and <sup>13</sup>C NMR data of compound **A** in d<sub>4</sub>-methanol with 0.1% TFA were in close agreement with those found in the literature for the known compound guttiferone A (**2.7**) (Table 2.1).<sup>12</sup> Therefore based on the similarity of the <sup>1</sup>H and <sup>13</sup>C NMR spectra with those found in the literature and the MS information compound **A** was determined to be guttiferone A (**2.7**).



2.7 Guttiferone A

Table 2.1  $^1\text{H}$  and  $^{13}\text{C}$  NMR data for compound A and guttiferone A.

Position	Guttiferone A <sup>a</sup>		Compound A <sup>a</sup>	
	$^{13}\text{C}$ NMR data	$^1\text{H}$ NMR data	$^{13}\text{C}$ NMR data	$^1\text{H}$ NMR data
1	195.4		195.5	
2	117.7		117.8	
3	195.1		195.1	
4	68.8		68.8 <sup>b</sup>	
5	51.9		51.9	
6	41.1	1.83 m	41.1	1.86 m
7	40.1	1.97 dd (14.3, 7.1) 2.09 dd (14.3, 1.2)	40.1	1.98 dd (14.1, 7) 2.08 m
8	62.1		62.1 <sup>b</sup>	
9	209.5		209.6	
10	195.5		195.6	
11	129.3		129.4	
12	117.3	7.16 d (2.2)	117.4	7.16 d (2.2)
13	146.1		146.2	
14	152.5		152.6	
15	115.1	6.69 d (8.3)	115.2	6.69 d (8.5)
16	125.0	6.97 dd (8.4, 2.2)	125.0	6.97 dd (8.5, 2.2)
17	26.6	2.62 dd (13.8, 4.9) 2.66 dd (13.8, 8.8)	26.6	2.62 d (13.3) 2.67 dd (13.3, 8.9)
18	120.7	4.92 m	120.8	4.93 m
19	135.6		135.6	
20	26.0	1.63 s	26.0	1.64 s
21	18.2	1.67 s	18.2	1.67 s
22	19.7	1.24 s	19.6	1.25 s
23	36.9	1.20 ddd (14.2, 10.4, 6.5) 1.39 ddd (14.4, 10.1, 6.2)	36.9	1.20 m 1.39 m
24	29.8	2.06 m 2.09 m	29.8	2.08 m 2.08 m

<b>25</b>	125.4	4.88 ddq (7.0, 7.0, 1.3)	125.5	4.88 m
<b>26</b>	133.7		133.8	
<b>27</b>	26.3	1.64 d (1.3)	26.3	1.65 s
<b>28</b>	18.2	1.47 s	18.1	1.47 s
<b>29</b>	32.0	2.44 dd (14.3, 6.6)	32.0	2.45 dd (13.8, 6.3)
		2.50 dd (14.3, 8.0)		2.50 dd (14.0, 8.0)
<b>30</b>	120.8	5.20 ddq (8.0, 6.6, 1.2)	120.8	5.19 ddd (6.6, 6.6, 1.2)
<b>31</b>	135.7		135.7	
<b>32</b>	26.3	1.71 d (1.2)	26.3	1.72 s
<b>33</b>	18.3	1.67 s	18.3	1.67 s
<b>34</b>	23.7	1.87 m	23.6	1.87 m
<b>35</b>	125.1	5.07 ddq (7.3, 7.2, 1.2)	125.1	5.08 dddd (7.1, 7.1, 1.4, 1.4)
<b>36</b>	132.8		132.9	
<b>37</b>	25.9	1.67 s	25.9	1.67 s
<b>38</b>	17.7	1.58 d (1.2)	17.7	1.59 s

<sup>a</sup>Recorded in CD<sub>3</sub>OD with 0.1% TFA. <sup>b</sup>Values from HMBC.

### 2.2.3 Structure Elucidation of Compound B

Compound **B** was isolated as a yellow amorphous solid. Its high-resolution positive ion FAB-MS indicated a molecular formula of C<sub>43</sub>H<sub>58</sub>O<sub>6</sub> (*m/z* 671.4332 [M+1]). The molecular weight and fragment ions observed at *m/z* 601, 533, 464, 395, and 325 indicated the presence of one additional isoprene unit as compared with guttiferone A.

The <sup>1</sup>H NMR spectrum of **B** in d<sub>4</sub>-methanol with 0.1% TFA revealed the presence of one aliphatic CH<sub>3</sub> (δ 0.82(s)) and nine allylic CH<sub>3</sub>'s (δ 1.56, 1.56, 1.59(s), 1.62(s), 1.64(d, *J*=0.9 Hz) 1.66(s), 1.67(s), 1.69(s), 1.70(s)). There were four signals due to vinylic protons (δ 5.00(m), 5.04(m), 5.05(m), 5.11(m)), and signals for an AMX spin system due to three aromatic protons (δ 6.68(d, *J*=8.3 Hz), 6.95(dd, *J*=8.3, 2.1 Hz), 7.20(d, *J*=2.1 Hz)). Overall the <sup>1</sup>H NMR spectrum was very similar to that of guttiferone A, and combined with the MS data led to the conclusion that compound **B** was a guttiferone analog.

The <sup>13</sup>C NMR spectrum in d<sub>4</sub>-methanol with 0.1% TFA was also similar to that of guttiferone A. However, it contained thirty-eight signals, in contrast to the thirty-five

observed with guttiferone A. It also appeared to have two overlapping methyl carbon signals ( $\delta$  26.3), as did guttiferone A.  $^{13}\text{C}$  NMR and DEPT 135 spectra indicated that the signals corresponding to the two saturated quaternary carbons that were missing in guttiferone A were also missing in compound **B**. It was also evident that only two carbonyl signals were present. An examination of the DEPT 135 spectrum combined with HMQC and HMBC provided the number and types of carbons in compound **B**. The DEPT 135 spectrum indicated that there were ten methyls ( $\delta$  16.3, 16.5, 17.8, 17.9, 18.2, 18.3, 25.9, 26.0, 26.3, 26.3) and eight methylenes ( $\delta$  25.2, 26.5, 27.5, 29.9, 31.6, 37.4, 40.8, 43.0). The  $^{13}\text{C}$  data also contained signals for one methine ( $\delta$  41.8) and one saturated quaternary carbon ( $\delta$  51.4). The other two saturated quaternary carbons were located via HMBC correlations at  $\delta$  62.7 and 68.8. Also present were signals for nineteen unsaturated carbons; of these nineteen signals, eight were due to protonated vinylic carbons, nine were due to quaternary vinylic carbons, and two were due to carbonyl carbons. Comparison of the  $^{13}\text{C}$  NMR spectrum of compound **B** with that of guttiferone A indicated that two carbonyl carbon signals were missing. Based on HMBC correlations and chemical shift the two missing carbonyls were identified as the ones in the keto-enol group. Their location was determined based on  $^{13}\text{C}$  NMR data after the solvent was changed as discussed below.

The structure of compound **B** was further determined by examining the HMBC and NOESY data. The assignment of the correlations in the HMBC spectrum was not a trivial matter. The overlap of several signals in the  $^1\text{H}$  NMR spectrum made assigning correlations difficult.

The single aliphatic methyl group was chosen as the starting point to examine the HMBC correlations. Two quaternary carbons ( $\delta$  51.4 and 68.8), a methylene carbon ( $\delta$  37.4) and a methine carbon ( $\delta$  41.8) all correlated to the aliphatic methyl ( $\delta$  0.82/16.3). Because it was a singlet in the  $^1\text{H}$  NMR spectrum, the aliphatic methyl group must be attached to a quaternary carbon. This allowed the construction of fragment 1 (Figure 2.4).

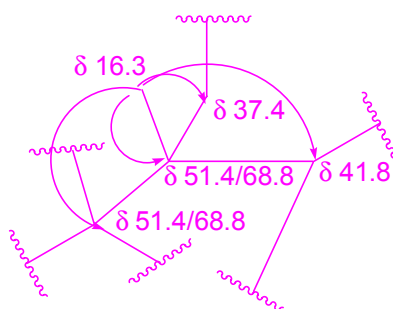


**Figure 2.4** HMBC fragment 1.

A carbonyl carbon ( $\delta$  209.0), two quaternary carbons ( $\delta$  68.8 and 135.0), and a methine carbon ( $\delta$  121.3) all correlated to methylene protons at 2.64 and 2.72 ppm ( $\delta$  26.5 in the  $^{13}\text{C}$  NMR spectrum). The proton on the methine carbon at  $\delta$  121.3 was shown by an HMQC spectrum to resonate at 4.8 ppm, and this proton showed HMBC correlations with two methyl carbons at 18.3 and 26.3 ppm. The placement of these methyls and the following ones were determined based on chemical shift and NOESY correlations. These correlations could thus be assembled to give fragment 2 (Figure 2.5).

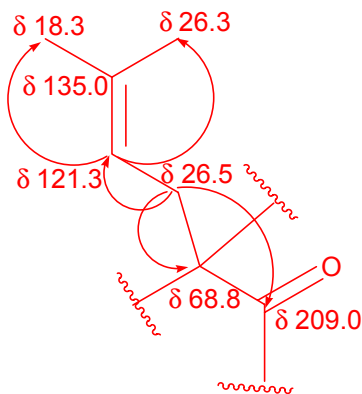


**Figure 2.5** HMBC fragment 2.

A set of correlations to a second pair of methylene protons at 2.44 and 2.52 ppm ( $\delta$  31.6 in  $^{13}\text{C}$  NMR spectrum) was observed for a carbonyl carbon ( $\delta$  209.0), two quaternary carbons ( $\delta$  62.7 and 135.5), a methine carbon ( $\delta$  120.9), and a methylene carbon ( $\delta$  43.0). In similar fashion to fragment 2 a methine carbon ( $\delta$  120.9) was found to resonate at 5.11 ppm in the HMQC spectrum and that proton showed correlations to two methyl carbons ( $\delta$  18.2 and 26.3) in the HMBC spectrum. These correlations were used to produce fragment 3 (Figure 2.6)

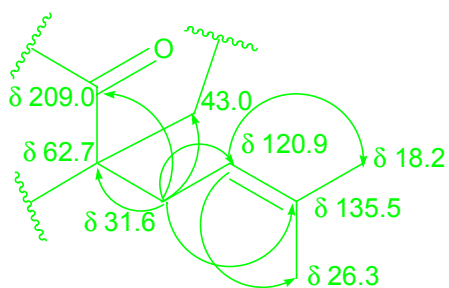


**Figure 2.6** HMBC fragment 3.

In a fourth fragment a methylene carbon ( $\delta$  37.4), a methine carbon ( $\delta$  125.5), and a quaternary carbon ( $\delta$  132.5) all correlated to a set of methylene protons at 1.97 ppm ( $\delta$  25.2 in the  $^{13}\text{C}$  NMR spectrum). There was also a correlation from a methyl carbon ( $\delta$  17.9) to the methine proton ( $\delta$  5.05/125.5). A second methyl carbon ( $\delta$  25.9) was correlated to the protons of the first methyl group ( $\delta$  1.59/17.9). These correlations made up fragment 4 (Figure 2.7).

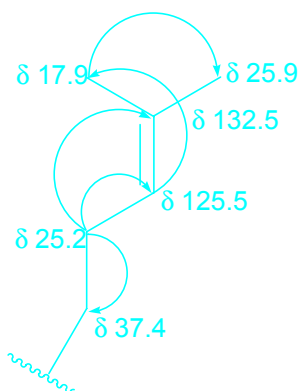


**Figure 2.7** HMBC fragment 4.

Correlations for fragment 5 were observed from a methyl carbon ( $\delta$  16.5) and a methylene carbon ( $\delta$  40.8) to a methine proton ( $\delta$  5.00/123.8). A quaternary carbon ( $\delta$  138.1) and a methyl carbon ( $\delta$  16.5) were correlated to methylene protons ( $\delta$  1.97/40.8). The methylene carbon ( $\delta$  40.8) was also correlated to another set of methylene protons ( $\delta$  2.07/27.5). That methylene carbon ( $\delta$  27.5) and a methyl carbon ( $\delta$  26.0) were correlated to a methine proton ( $\delta$  5.04/125.2). A methyl carbon ( $\delta$  17.8) and a quaternary carbon ( $\delta$  132.3) were subsequently correlated to the same methyl protons ( $\delta$  1.64/26.0). These correlations allowed fragment 5 (Figure 2.8) to be constructed.



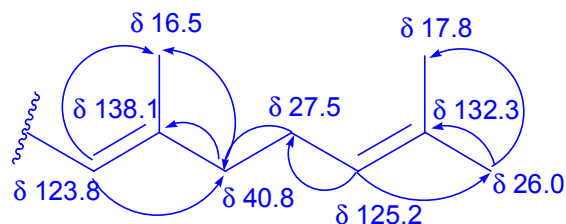


**Figure 2.8** HMBC fragment 5.

The sixth and final HMBC fragment (Figure 2.9) made up the aromatic ring system. For this fragment, correlations from a methine carbon ( $\delta$  124.9), a carbonyl carbon ( $\delta$  196.5) and a quaternary carbon ( $\delta$  152.5) to a methine proton ( $\delta$  7.20/117.3) were observed. Correlations from a carbonyl carbon ( $\delta$  196.5) and a quaternary carbon ( $\delta$  152.5) were observed for another methine proton ( $\delta$  6.95/124.9). The last set of correlations for this fragment were from two quaternary carbons ( $\delta$  146.3 and 130.2) to the final methine proton ( $\delta$  6.68/115.1).

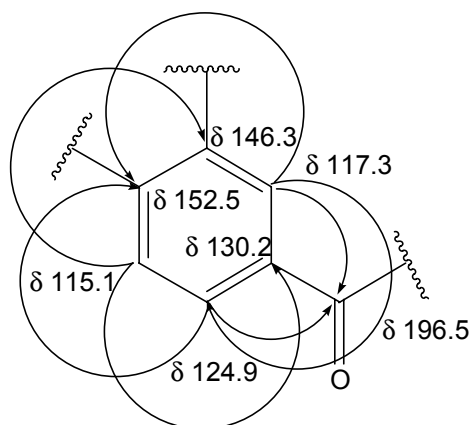


**Figure 2.9** HMBC fragment 6.

These fragments were then pieced together based on further HMBC correlations. Fragment 2 was connected to fragment 3 through the shared correlation to the carbonyl carbon at  $\delta$  209.0. Fragment 1 was connected to fragment 2 through the shared quaternary ( $\delta$  68.8) correlation. Fragment 4 was connected to fragment 1 through a shared correlation to the methylene carbon at  $\delta$  37.4. Fragment 1 and fragment 3 were connected via correlations to the methylene carbon at  $\delta$  43.0. A quaternary carbon ( $\delta$  51.4) and a carbonyl carbon ( $\delta$  209.0) were correlated to a pair of methylene protons ( $\delta$  2.07/43.0). The correlations of the two methylene groups ( $\delta$  26.5 and 43.0) established the positions of the two quaternary carbons ( $\delta$  51.4 and 68.8). The fifth fragment was connected to fragment 1 through a shared correlation to the methine carbon at  $\delta$  41.8 to give fragment 7 (Figure 2.10).

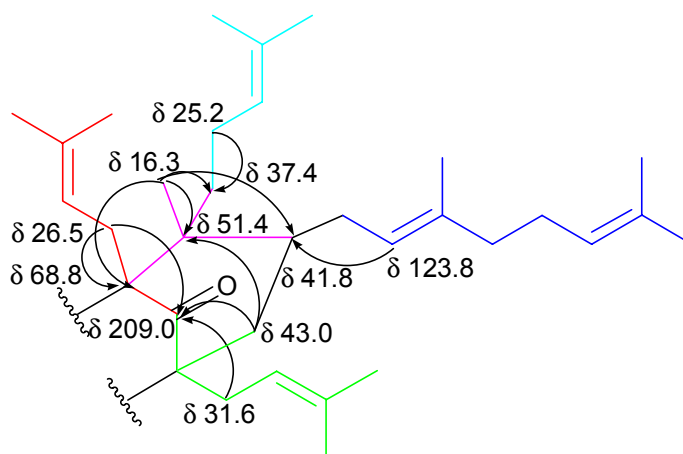


**Figure 2.10** HMBC fragment 7.

Since the mass spectrum and  $^1\text{H}$  and  $^{13}\text{C}$  NMR data all indicated that compound **B** was an analog of guttiferone A that contained an additional isoprene unit, the key

correlation between fragment 1 and fragment 5 provided information on the placement of the extra isoprene unit. Finally fragment 6 was connected to fragment 7 based on the known structure of guttiferone A. It was not possible to make this connection on the basis of HMBC correlations due to the lack of protonated carbons on that section of the molecule. The hydroxyl groups were placed on the aromatic ring on the basis of chemical shift values, HMBC correlations, and comparison to guttiferone A (Figure 2.11).

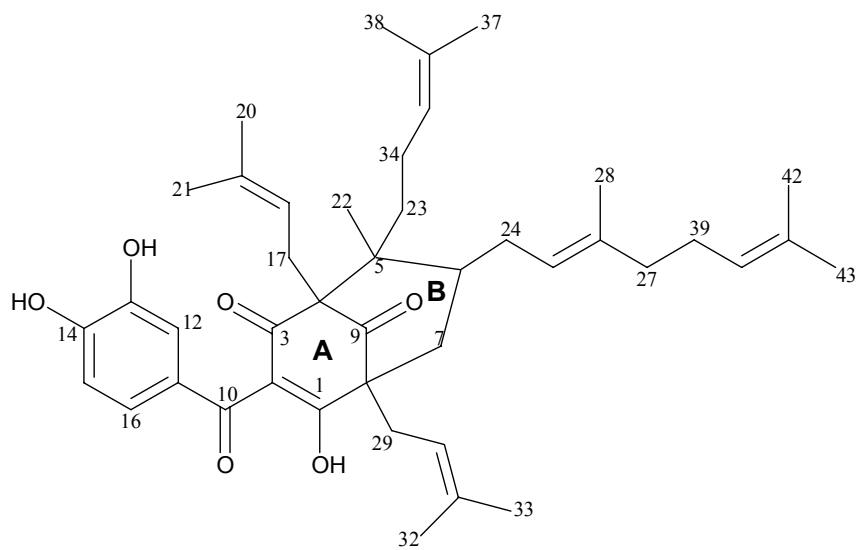


**Figure 2.11** Compound **B** with carbon numbering.

The overlap of several signals in the  $^1\text{H}$  NMR spectrum when  $\text{d}_4$ -methanol was used as the solvent made some of the correlations difficult to determine. In order to obtain better correlations, pyridine was used to induce an aromatic solvent induced shift (ASIS), since this technique spreads out the signals in the  $^1\text{H}$  NMR spectrum. It was hoped that this would result in fewer overlapping signals, and therefore lead to clearer

correlations. The resulting HMBC correlations proved helpful in further confirming the structure of compound **B**. It was also noted that the HSQC experiment was capable of giving much clearer  $^1J_{\text{CH}}$  correlations than the HMQC, and thus HSQC was used to provide the following  $^1J_{\text{CH}}$  correlations

The  $^1\text{H}$  NMR spectrum of **B** in  $\text{d}_5$ -pyridine provided HSQC correlations for position 24. These correlations were not seen when the spectrum was obtained in  $\text{d}_4$ -methanol with 0.1% TFA, since the proton signals were presumably overlapped with the allylic methyl proton signals. However, in  $\text{d}_5$ -pyridine the proton signals were resolved making it possible to assign the protons of C-24 to  $\delta$  1.96 and 2.30 by HSQC correlations to C-24 at  $\delta$  29.9. Two methine carbons ( $\delta$  41.2 and 124.3) were correlated to the C-24 protons in the HMBC spectrum. It was also possible to assign additional correlations to positions 17 ( $\delta$  3.04 and 3.11/26.8) and 29 ( $\delta$  2.92/31.7). Two carbonyl carbons ( $\delta$  187.5 and 191.0) were correlated to positions 17 and 29 respectively (Figure 2.12).

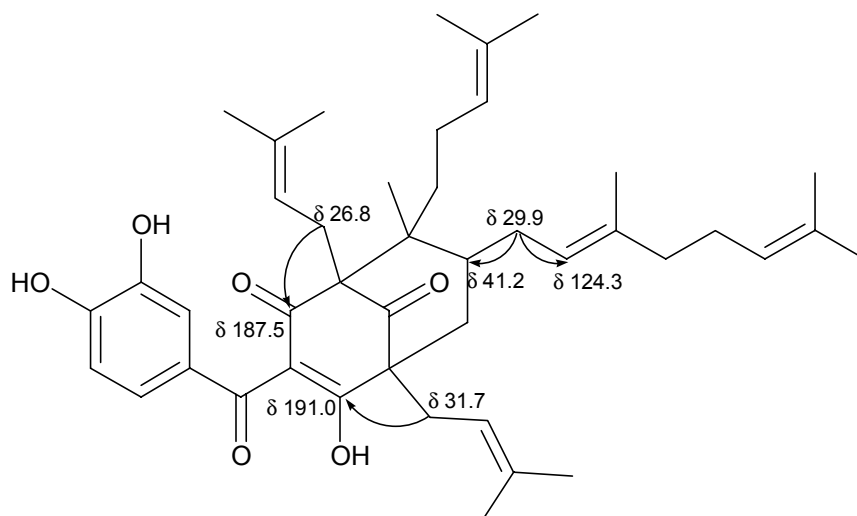


**Figure 2.12** HMBC correlations of compound **B** in  $\text{d}_5$ -pyridine.

Overall pyridine appeared to be a much better solvent choice for the guttiferones than methanol, the solvent typically used for literature values. In addition to causing an ASIS that allowed for easier correlations, the ability to avoid overlap of the water signal, when dry solvent is used, with those of the vinyl protons was also advantageous. Conversely, because pyridine is basic and the guttiferones are acidic, it is possible that compound **B** is deprotonated. This could explain the improvement in the spectra. However, examination of the  $^1\text{H}$  and  $^{13}\text{C}$  NMR spectra showed no evidence of pyridinium signals.

The positioning of the allylic methyl groups and the stereochemistry of the double bond at C25 were determined based on chemical shift data and NOESY spectrum correlations. The geometry of the double bond at C25 was determined to be *E* based on a chemical shift of  $\delta$  16.7 and a NOESY correlation between the C25 methine ( $\delta$  5.51) and the C27 methylene ( $\delta$  2.01). The positions of the remaining methyl groups were determined based on similar NOESY correlations and literature evidence that the methyl groups in the *trans* position have chemical shifts of about  $\delta$  26 whereas the *cis* methyl groups have chemical shifts ranging between  $\delta$  16 and 19.<sup>12</sup> Determination of the relative configuration of **B** was not straightforward. Due to the overlap of the methine C6 signal with the methylene C24 signal it was not possible to determine the relative stereochemistries at C4, C5, C6, or C8, in  $\text{d}_4$ -methanol. In  $\text{d}_5$ -pyridine it was possible to obtain much clearer NOESY correlations. NOESY correlations from the C22 methyl ( $\delta$  1.01) to the C17 methylene ( $\delta$  3.04) and of the C23 methylene ( $\delta$  1.99) to the C17 methylene ( $\delta$  3.11) indicated that the C17 carbon bisected the C22 and C23 carbons. Correlations from the C22 ( $\delta$  1.01) to the C24 methylene ( $\delta$  1.96) and of the C23

methylene ( $\delta$  1.99) to the C24 methylene ( $\delta$  2.30) indicated that the C24 methylene also bisected the C22 and C23 carbons. Correlations from the C22 methyl ( $\delta$  1.01) to the C7 methylene ( $\delta$  ~1.76), combined with the previously mentioned correlation between C22 and C24 indicates that the C22 carbon bisects the C7 and C24 carbons. The C7 methylene was also observed to correlate to the C24 and C29 methylenes.

Because the two non-aromatic rings form a bicyclo[3.3.1]nonane ring system, C17 and C29 must be equatorial to the B ring. In order for C17 and C24 to bisect C22 and C23, and for C22 to bisect C7 and C24, the B ring must be in the chair conformation. This is the only conformation that accounts for the observed NOESY correlations and also explains the lack of correlations between the C22 methyl and the C6 methine, and the C23 methylene and the C7 methylene. The correlation between the C22 methyl and the C7 methylene (one proton only) indicates that both groups are axial. Such a correlation would be possible in the boat conformation, but one would then expect to see correlations from C22 methyl and C23 methylene to the C6 methine. Additionally in the boat conformation the C22 methyl and C23 methylene would not both correlate to the C17 methylene. Only the group that was in the axial position would be capable of a NOESY correlation. Thus, based on the NOESY spectra, the ring is in the chair conformation with all of the isoprene groups in equatorial positions (Figure 2.13).

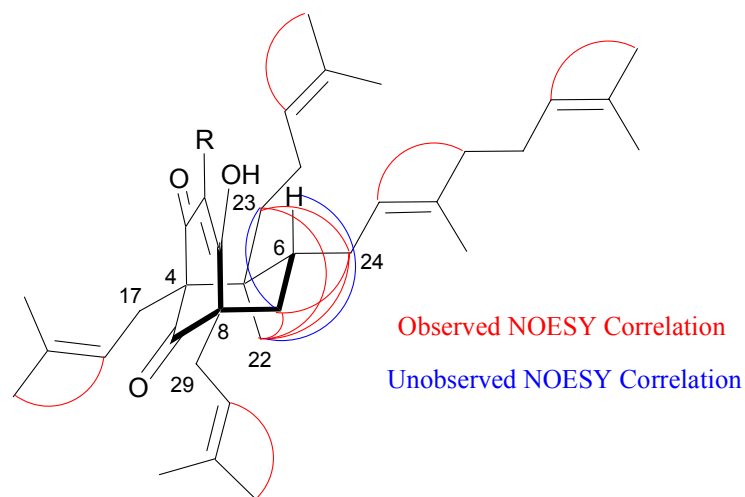


**Figure 2.13** Selected NOESY correlations for compound **B**.

Unfortunately it was not possible to examine the coupling constants of the C6 methine and C7 methylene protons due to the lack of a clearly defined splitting pattern and overlap with other signals. It was, however, possible to compare the NOESY correlations of compound **B** to guttiferone A. A NOESY experiment was run on the sample of guttiferone A previously isolated, to verify the correlations found in the literature.<sup>12</sup> The results matched those found in the literature. Just as in compound **B**, guttiferone A had NOESY correlations between the C22 methyl and C23 methylene to the C17 methylene, between the C7 methylene and C29 methylene, between the C22 methyl and C23 methylene, and between the C22 methyl and C24 methylene. However, it differed in that the C23 methylene showed no correlation to the C24 methylene, and the C23 methylene, not the C22 methyl, correlated to one of the C7 methylene protons. It also differed in that both the C22 methyl and the C23 methylene correlated to the C6 methine (Figure 2.14).

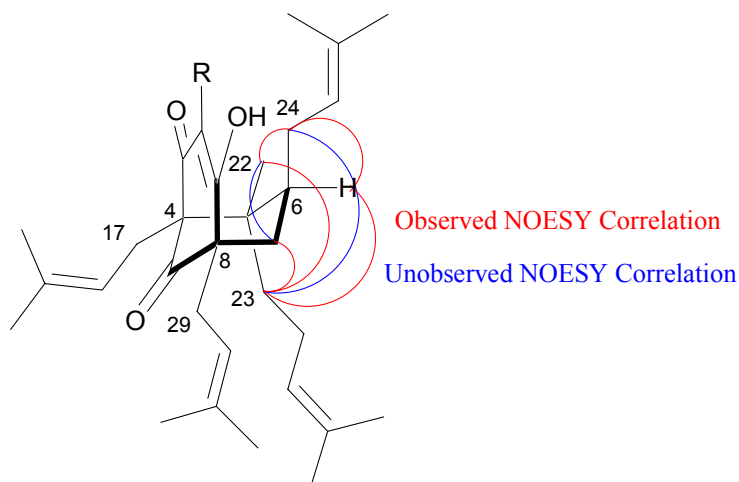


**Figure 2.14** Selected NOESY correlations for guttiferone A (2.7).

The presence of NOESY correlations from the C22 methyl and the C23 methylene to the C17 methylene indicated that the B ring is in the chair position. The C23 methylene must be axial based on the NOESY correlation to the C7 methylene. The lack of a NOESY correlation from the C23 methylene to the C24 methylene indicated that the C24 group was axial. In the axial position the NOESY correlation that was observed between the C22 methyl and the C24 methylene would be possible. Thus the NOESY correlations place the C23 and the C24 groups in axial positions with the B ring in the chair position.

As a means of further confirming the relative stereochemistry of guttiferone A other possible structures were examined using MM2 minimized 3-D structures. Because it was evident that the B ring was in the chair configuration and the C23 group was axial based on the aforementioned NOESY correlations, it was only necessary to examine two structures.

The first structure examined was with the C24 group in the equatorial position (Figure 2.15). It was minimized ( $E = 43.1458$ ) and the proton distances were compared



to the observed NOESY correlations (Table 2.2). The distances indicated that NOESY correlations would be observed from the C22 methyl to the C6 methine, to the C17 methylene, to the C23 methylene, and to the C24 methylene, and from the C23 methylene to the C7 methylene, to the C17 methylene, and to the C24 methylene. These differ from the observed NOESY correlations in that no correlation was observed between the C23 methylene and the C24 methylene. It was also possible to examine the coupling constant observed for the axial proton attached to C7. Based on the 3-D structure the torsion angle between the C6 methine proton and the axial C7 proton was  $168^\circ$ . Based on the Karplus correlation the expected coupling constant would be approximately 12 Hz, much higher than the 7 Hz that was observed.

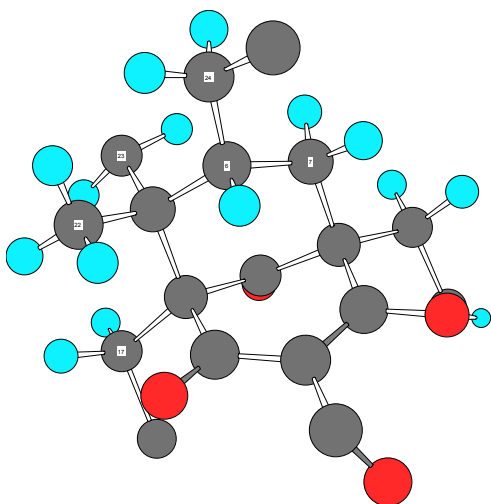


**Table 2.2** Distances in Å between selected protons for the C23 axial, C24 equatorial configuration.

	C6	C7	C17	C22	C23	C24
C22	2.4	4.6	2.1	—	2.8	2.1
C23	3.8	2.3	2.1	2.8	—	2.8

**Figure 2.15** C23 axial/C24 equatorial chair configuration of guttiferone A.

The second structure was with the C24 group in the axial position (Figure 2.16). It was minimized ( $E = 47.6345$ ) and the proton distances were examined for possible NOESY correlations (Table 2.3). The distances indicated that NOESY correlations

would be observed from the C22 methyl to the C6 methine, to the C17 methylene, to the C23 methylene, and to the C24 methylene, and from the C23 methylene to the C6 methine, to the C7 methylene, to the C17 methylene, and to the C22 methyl. These distances matched the observed NOESY correlations. Again the coupling constant for the axial C7 proton was examined. The torsion angle between the C6 methine proton and the axial C7 proton was  $41^\circ$ . Based on the Karplus correlation the expected coupling constant would be approximately 7 Hz, matching the coupling constant that was observed.

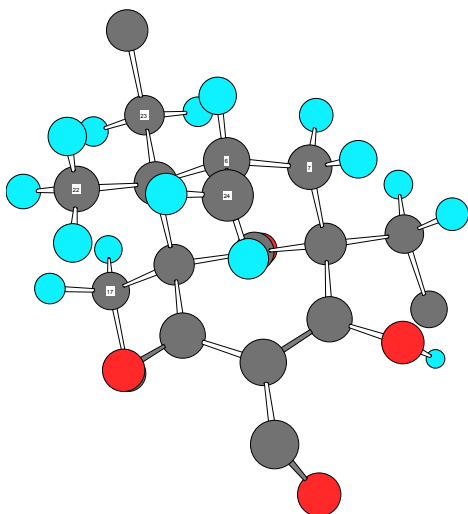


**Table 2.3** Distances in Å between selected protons for the C23, C24 axial configuration.

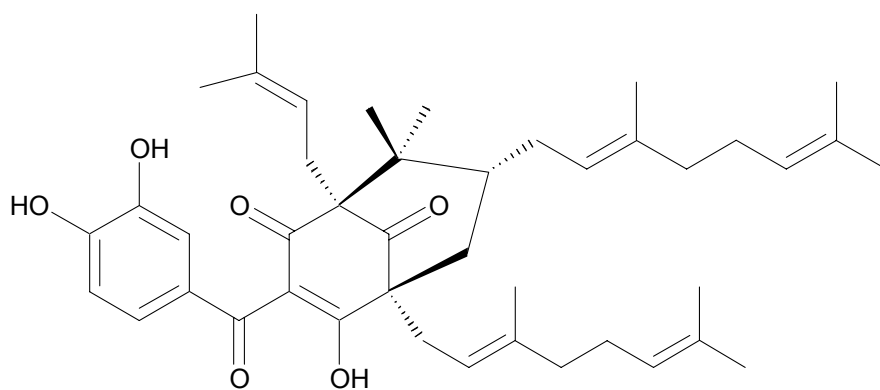
	C6	C7	C17	C22	C23	C24
C22	2.6	4.6	2.2	—	2.4	2.2
C23	2.9	2.4	2.2	2.4	—	4.8

**Figure 2.16** C23/C24 axial chair configuration of guttiferone A.

Initially it is somewhat surprising that chair conformation with the C23 and C24 groups in axial positions would be favored over the boat conformation with the groups in equatorial positions. However, construction of the 3-D model of the boat conformation ( $E = 50.1181$ ) of guttiferone A reveals that it is higher in energy than the chair conformation ( $E = 47.6345$ ). Examination of the boat conformation reveals the possibility of significant steric interaction with the C17 group.

Based on the NOESY correlations and the coupling constant datum the stereochemistry at C5 and C6 in guttiferone A, with both substituents in axial positions, are the opposite of those found in compound **B**.

The optical rotation data lends further support to the claim that compound **B** contains the opposite stereochemistry at C5 and C6 compared to guttiferone A. Guttiferone A has an optical rotation of  $+34^\circ$  while compound **B** has an optical rotation of  $-25^\circ$ .<sup>12</sup> If the difference between the two compounds were only the addition or removal of an isoprene unit then one would expect the change in optical rotation to be small. However, the fact that they have nearly opposite optical rotations indicates that there is a major change in the stereochemistry of compound **B** compared to that of guttiferone A (**2.7**). There are no other guttiferones reported in the literature with the same stereochemistry as that proposed for compound **B**. However, guttiferone B (**2.8**) has the same stereochemistry at C6 as that proposed for compound **B**, but lacks the stereocenter at C5. Guttiferone B (**2.8**) has an optical rotation of  $-44^\circ$ .<sup>12</sup> Though guttiferone B (**2.8**) is not identical to compound **B** it is similar, and the optical rotation is in the same range as that of compound **B**.



**2.8 Guttiferone B**

As a final means of confirming the relative stereochemistry of compound **B** several possible configurations were examined using MM2 minimized 3-D structures. There are sixteen possible isomers if the stereochemistry at C5 and C6 are varied and both chair and boat conformations are allowed. However, it was possible to reduce the number of possible configurations by requiring that the configurations allow for a NOESY correlation between the C22 methyl and one of the C7 methylene protons (one of the observed NOESY correlations). That resulted in four possible configurations, two chair conformations and two boat conformations. Those configurations were minimized using CambridgeSoft's Chem3D Pro 6.0 MM2 minimize energy operation. The distances between the appropriate protons were then examined. A distance of less than 3 Å was considered small enough to provide a NOESY correlation and a distance greater than 3 Å was not considered small enough to provide a NOESY correlation.

The two boat conformations had the highest energy. The boat conformation of compound **B** with the C23 and C24 groups in the equatorial position (Figure 2.17) was minimized ( $E = 60.7802$ ). The minimization showed that NOESY correlations should be observed from the C22 methyl to the C7 methylene and to the C23 methylene, and from the C23 methylene to the C6 methine, to the C17 methylene, to the C22 methylene, and to the C24 methylene. It also showed that NOESY correlations should not be seen from the C22 methyl to the C6 methine, to the C17 methylene, and to the C24 methylene, and from the C23 methylene to the C7 methylene (Table 2.4). However, no NOESY correlations were observed from the C23 methylene to the C6 methine for compound **B**. Also NOESY correlations were observed from the C22 methyl to the C17 methylene and to the C24 methylene for compound **B**.

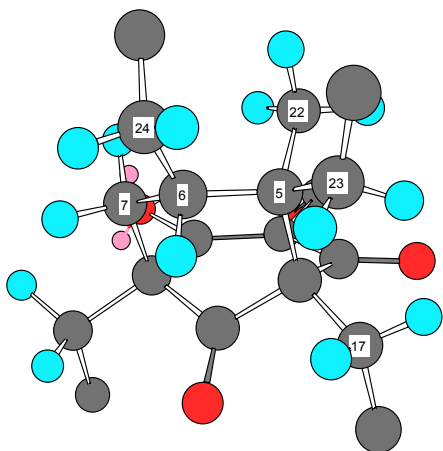


**Figure 2.17** C23/C24 equatorial boat configuration of compound **B**.

**Table 2.4** Distances in Å between selected protons for the C23, C24 equatorial boat configuration.

	C6	C7	C17	C22	C23	C24
C22	3.8	2.3	3.6	—	2.7	3.4
C23	2.5	4.7	2.3	2.7	—	2.7

The second boat configuration of compound **B** had the C23 group in the equatorial position and the C24 group in the axial position (Figure 2.18). It was minimized to give an energy of 59.1062. The minimization showed that the C22 methyl should show NOESY correlations to the C6 methine, to the C7 methylene, and to the C23methylene. C23 should show NOESY correlations to the C17 methylene, to the C22 methylene, and to the C24 methylene. There should be no NOESY correlations observed from the C22 methyl to the C17 methylene and to the C24 methylene (Table 2.5). However, no NOESY correlations were observed from the C22 methyl to the C6 methine for compound **B**. In addition NOESY correlations were observed from the C22 methyl to the C17 methylene and to the C24 methylene for compound **B**.

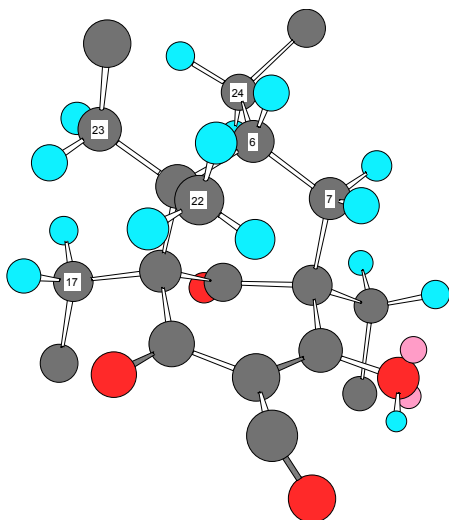


**Figure 2.18** C23 equatorial/C24 axial boat configuration of compound **B**.

**Table 2.5** Distances in Å between selected protons for the C23 equatorial, C24 axial boat configuration.

	C6	C7	C17	C22	C23	C24
C22	2.3	2.3	3.4	—	2.4	4.2
C23	3.4	4.9	2.1	2.4	—	2.2

The chair conformation with the C23 methylene in the equatorial position and the C24 methylene in the axial position was minimized to give an energy of 52.4862 (Figure 2.19). This minimization was examined and found to indicate NOESY correlations from the C22 methyl to the C6 methine, to the C7 methylene, to the C17 methylene, and to the C23 methylene. The C23 methylene should have produced NOESY correlations between the C6 methine, the C17 methylene, the C22 methyl, and the C24 methylene (Table 2.6). However, the lack of any indication of a NOESY correlation between the C22 methyl and the C24 methylene and the indication of NOESY correlations from the C22 methyl and the C23 methylene to the C6 methine are in contrast to the NOESY correlations observed for compound **B**.

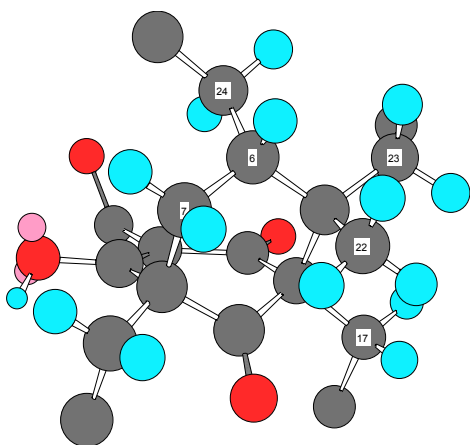


**Figure 2.19** C23 equatorial/C24 axial chair configuration of compound **B**.

**Table 2.6** Distances in Å between selected protons for the C23 equatorial, C24 axial chair configuration.

	C6	C7	C17	C22	C23	C24
C22	2.3	2.2	2.1	—	2.3	4.1
C23	2.5	4.4	2.5	2.3	—	2.5

The final configuration examined was the chair conformation with the C6 and C23 methylenes in equatorial positions (Figure 2.20). It was minimized to give an energy of 47.6109. The observed distances were found to match the NOESY correlations for compound **B** (Table 2.7). The data obtained from the 3-D structures were summarized in Table 2.8.

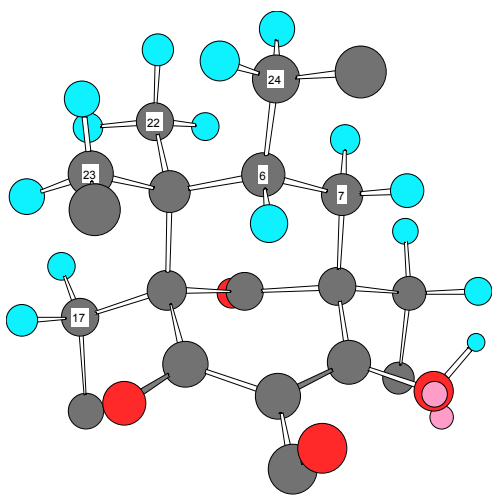


**Figure 2.20** C23/C24 equatorial chair configuration of compound **B**.

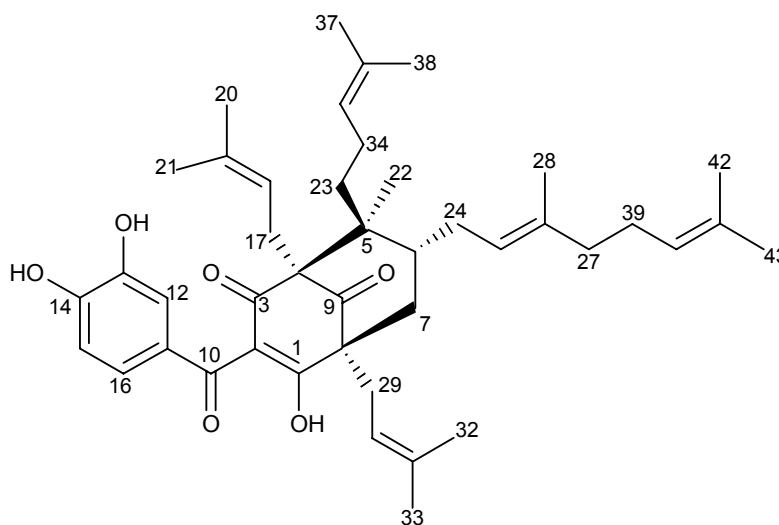
**Table 2.7** Distances in Å between selected protons for the C23, C24 equatorial chair configuration.

	C6	C7	C17	C22	C23	C24
C22	3.8	2.3	2.1	—	2.3	2.2
C23	3.4	4.5	2.2	2.3	—	2.7

**Table 2.8** Summary of expected and observed correlations.

	Figure 2.17	Figure 2.18	Figure 2.19	Figure 2.20	Experimental
<b>C22-C6</b>	–	✓	✓	–	–
<b>C22-C7</b>	✓	✓	✓	✓	✓
<b>C22-C17</b>	–	–	✓	✓	✓
<b>C22-C23</b>	✓	✓	✓	✓	✓
<b>C22-C24</b>	–	–	–	✓	✓
<b>C23-C6</b>	✓	–	✓	–	–
<b>C23-C7</b>	–	–	–	–	–
<b>C23-C17</b>	✓	✓	✓	✓	✓
<b>C23-C24</b>	✓	✓	✓	✓	✓

Thus the structure of compound **B** has been determined to be a novel  $C_{43}H_{58}O_6$  guttiferone analog. It contains an additional isoprene group when compared to guttiferone A, in that the isopentenyl group at C6 is replaced with a geranyl group. In addition, the stereochemistry at C5 and C6 is reversed as compared with guttiferone A (2.7). The compound is named guttiferone G (2.9) in continuation of the custom of naming guttiferone analogs with sequential letters of the alphabet.



**2.9 Guttiferone G (Compound B)**



**Table 2.9**  $^1\text{H}$  and  $^{13}\text{C}$  NMR data for compound **A** and compound **B**.

Position	Compound A <sup>a</sup>		Compound B <sup>b</sup>	
	$^{13}\text{C}$ NMR data	$^1\text{H}$ NMR data	$^{13}\text{C}$ NMR data	$^1\text{H}$ NMR data
1	195.5		191.0	
2	117.8		121.7	
3	195.1		187.5	
4	68.8 <sup>c</sup>		69.4	
5	51.9		49.7	
6	41.1	1.86 m	41.2	2.60 m
7	40.1	1.98 dd (14.1, 7) 2.08 m	41.9	1.76 m 2.48 dd (13.4, 4.4)
8	62.1 <sup>c</sup>		62.9	
9	209.6		210.2	
10	195.6		196.6	
11	129.4		130.2	
12	117.4	7.16 d (2.2)	117.3	7.86 d (2.1)
13	146.2		146.3	
14	152.6		152.5	
15	115.2	6.69 d (8.5)	115.1	7.16 d (8.3)
16	125.0	6.97 dd (8.5, 2.2)	124.9	7.62 dd (8.3, 2.1)
17	26.6	2.62 d (13.3) 2.67 dd (13.3, 8.9)	26.8	3.04 dd (14.1, 5.9) 3.11 dd (14.1, 7.0)
18	120.8	4.93 m	123.4	5.51 ddd (5.5, 5.5, 1.4)
19	135.6		132.5	
20	26.0	1.64 s	26.4	1.60 s
21	18.2	1.67 s	18.7	1.80 s
22	19.6	1.25 s	16.6	1.01 s
23	36.9	1.20 m 1.39 m	37.1	1.99 m
24	29.8	2.08 m 2.08 m	29.9	1.96 m 2.30 m
25	125.5	4.88 m	124.3	5.27 m
26	133.8		137.2	
27	26.3	1.65 s	40.3	2.01 m
28	18.1	1.47 s	16.7	1.68 s
29	32.0	2.45 dd (13.8, 6.3) 2.50 dd (14.0, 8.0)	31.7	2.92 d (7.1)
30	120.8	5.19 ddd (6.6, 6.6, 1.2)	122.3	5.73 m
31	135.7		133.6	
32	26.3	1.72 s	26.4	1.68 s
33	18.3	1.67 s	18.6	1.76 s
34	23.6	1.87 m	25.0	2.28 m 2.55 m
35	125.1	5.08 dddd (7.1, 7.1, 1.4, 1.4)	126.1	5.22 m
36	132.9		131.4	
37	25.9	1.67 s	26.1	1.66 s
38	17.7	1.59 s	18.2	1.66 s
39			27.3	2.12 m
40			125.1	5.18 m
41			131.7	
42			26.2	1.72 d (0.9)
43			18.1	1.57 s

<sup>a</sup>Recorded in  $\text{CD}_3\text{OD}$  with 0.1% TFA. <sup>b</sup>Recorded in  $\text{d}_5\text{-pyridine}$ . <sup>c</sup>Values from HMBC.

#### 2.2.4 The Structure Elucidation of Compound C

Compound **C** was isolated as colorless needles from CH<sub>2</sub>Cl<sub>2</sub> and MeOH. High-resolution positive ion FAB MS indicated a molecular formula of C<sub>30</sub>H<sub>50</sub>O ([M+H]<sup>+</sup> 427.3931).

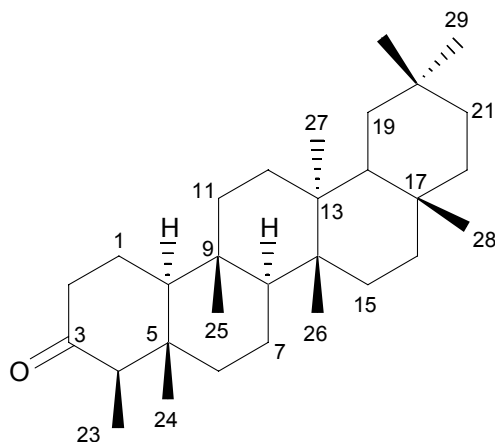
The structure of compound **C** was determined by examination of <sup>1</sup>H NMR, <sup>13</sup>C NMR, and APT spectra, and a comparison of the <sup>1</sup>H and <sup>13</sup>C NMR data to that found in the literature (Table 2.10).<sup>17,18</sup> The <sup>1</sup>H NMR in CDCl<sub>3</sub> indicated the presence of eight methyl signals (δ 0.72(s), 0.86(s), 0.87(d (*J*=6.9 Hz)), 0.95(s), 0.99(s), 1.00(s), 1.04(s), 1.17(s)) in addition to numerous methylene and methine signals. There were no signals in the <sup>1</sup>H NMR spectrum to indicate the presence of any hydroxyl groups or the presence of any vinylic protons. The <sup>13</sup>C NMR and APT in CDCl<sub>3</sub> indicated the presence of 8 methyls, 11 methylenes, 4 methines, and 7 quaternary carbons, one of which was a ketone. After an examination of the literature it was determined that the molecular formula and <sup>13</sup>C NMR data of **C** most closely matched that of friedelin (**2.10**). Friedelin has been previously isolated from multiple *Garcinia* species.<sup>7,19</sup>

---

<sup>17</sup> Mahato, S. B.; Kundu, A. P. <sup>13</sup>C NMR Spectra of Pentacyclic Triterpenoids—A Compilation and some Salient Features. *Phytochemistry*. **1994**, *37*, 1517-1575.

<sup>18</sup> Klass, J.; Tinto, W. F.; McLean, S.; Reynolds, W. F. Friedelin Triterpenoids from *Peritassa compta*: Complete <sup>1</sup>H and <sup>13</sup>C Assignments by 2D NMR Spectroscopy. *J. Nat. Prod.* **1992**, *55*, 1626-1630.

<sup>19</sup> Spino, C.; Lal, J.; Sotheeswaran, S.; Aalbersberg, W. Three Prenylated Phenolic benzophenones from *Garcinia myrtifolia*. *Phytochemistry*. **1995**, *38*, 233-236.



### 2.10 Friedelin (Compound C)

**Table 2.10**  $^{13}\text{C}$  NMR data and selected  $^1\text{H}$  NMR data of friedelin and compound C.

Position	Friedelin (2.10) <sup>a</sup>		Compound C <sup>a</sup>	
	$^{13}\text{C}$ NMR	$^1\text{H}$ NMR	$^{13}\text{C}$ NMR	$^1\text{H}$ NMR
1	22.27	1.68, 1.96	22.28	1.68 dddd (26.1, 13.1, 13.1, 5.2) 1.96 m
2	41.51	2.28, 2.39	41.52	
3	213.17		213.25	
4	58.19	2.25	58.22	2.24 q (6.9)
5	42.13		42.15	
6	41.27	1.28, 1.75	41.28	1.74 m
7	18.23	1.37, 1.49	18.23	
8	53.08	1.39	53.09	
9	37.42		37.43	
10	59.45	1.53	59.47	
11	35.61	1.26, 1.46	35.62	
12	30.50	1.34, 1.34	30.50	
13	39.68		39.69	
14	38.28		38.29	
15	32.76	1.27, 1.46	32.76	
16	36.00	1.36, 1.57	36.00	
17	29.98		29.98	
18	42.77	1.56	42.78	
19	35.32	1.20, 1.38	35.33	1.20 dd (13.9, 5.8)
20	28.16		28.16	
21	32.40	1.30, 1.51	32.41	
22	39.24	0.94, 1.50	39.24	
23	6.83	0.87	6.82	0.87 d (6.9)
24	14.65	0.71	14.65	0.72 s
25	17.94	0.86	17.94	0.86 s
26	20.26	1.00	20.25	0.99 s/1.00 s
27	18.67	1.05	18.66	1.04 s
28	32.09	1.17	32.08	1.17 s
29	31.79	1.00	31.77	0.99 s/1.00 s
30	35.03	0.95	35.02	0.95 s

<sup>a</sup>Spectra collected in  $\text{CDCl}_3$ .

### 2.2.5 Biological Evaluation of Friedelin and Guttiferones A and G

Friedelin is a well-known triterpene that can be obtained from the processing of *Quercus suber* L. (Fagaceae) to produce cork. It has been reported to have diuretic activity.<sup>20</sup> It has not been reported to possess any cytotoxic activity, and indeed was inactive in the A2780 human ovarian cell line. It has recently been used as a starting material to produce several triterpenoid derivatives that do show some cytotoxicity.<sup>20</sup>

The guttiferones, as previously mentioned, have been shown to demonstrate anti-HIV, anti-bacterial, anti-oxidant, and cytotoxic activity. Guttiferone A specifically has been shown to possess anti-HIV activity in the NCI's primary anti-HIV screen. In the A2780 human ovarian cell line it was found to have weak cytotoxic activity ( $IC_{50} = 6.8 \mu\text{g/ml}$ ).

Guttiferone G, being a novel compound, has no previously reported activity. However, one would expect that it would exhibit similar activity to previously isolated guttiferones. In the A2780 human ovarian cell line it possessed a cytotoxic activity similar to that of guttiferone A ( $IC_{50} = 8.0 \mu\text{g/ml}$ ).

## 2.3 Experimental Section

**General Experimental Procedures.** Optical rotations were measured on a Perkin-Elmer 241 polarimeter. UV spectra were obtained using a Shimadzu UV-1201 spectrophotometer. IR spectra were obtained using a Midac M-Series FTIR spectrophotometer. Low resolution FABMS taken on a Fisons VG Quattro instrument.

---

<sup>20</sup> Moiteiro, C.; Justino, F.; Tavares, R.; Marcelo-Curto, M. J.; Florêncio, M. H.; Nascimento, M. S. J.; Pedro, M.; Cerqueira, F.; Pinto, M. M. M. Synthetic Secofriedelane and Friedelane Derivatives as Inhibitors of Human Lymphocyte Proliferation and Growth of Human Cancer Cell Lines in Vitro. *J. Nat. Prod.* **2001**, *64*, 1273-1277.

High resolution FABMS were taken on a JEOL HX-110 instrument. 1D and 2D NMR data collected on a JEOL Eclipse instrument at 500 MHz for proton and 125 MHz for carbon, or a Varian Inova instrument at 400 MHz for proton and 100 MHz for carbon. Thin layer chromatography was performed on Whatman MKC<sub>18</sub>F reversed phase TLC plates, and Sigma-Aldrich silica gel TLC plates. Column chromatography was performed using Sigma lipophilic Sephadex LH-20, and Whatman LRP2.

**Cytotoxicity Bioassay.** The A2780 human ovarian cell line was employed as an *in vitro* cytotoxicity assay as previously reported.<sup>21</sup>

**Plant Material.** The stems of *Garcinia macrophylla* Mart. (Clusiaceae = Guttiferae) were collected at 4°45'30" N, 56°52'50" W, elev. 50 m, in the province of Sipaliwini, which is a large inland province of Suriname, on August 7, 1995, by Randy Evans, Eric Bakboord, Steve Corso, and Sylva Koemar, of the Missouri Botanical Garden. A voucher specimen (EVANS 2397) can be found at the Missouri Botanical Garden (MO), and was identified by B. Hammel of the Missouri Botanical Garden. The plant was found growing in a primary lowland wet forest, in a dry streambed. It was a 20 m tall tree, and had stems and leaves with yellow latex. It had green buds that were about 5 mm in diameter, on pedicels of about 15 mm long.

**Extract Preparation.** The stems of *Garcinia macrophylla* were extracted with EtOAc followed by MeOH to give two crude extracts E950358 and M950358, respectively.

---

<sup>21</sup> Chapter 1 Bioassay Section.

**Bioassay Guided Fractionation and Isolation of Compounds.** Extract E950358 (500 mg) was taken for fractionation. It was partitioned between hexane and 80% aqueous MeOH. The aqueous methanol fraction was diluted with water to give a 50% aqueous MeOH fraction, which was further partitioned with CH<sub>2</sub>Cl<sub>2</sub>. The fractions were concentrated via rotary evaporation to give active hexane and dichloromethane fractions. The more active dichloromethane fraction was chromatographed over RP C-18, using aqueous MeOH gradient elution (60%-100%), to produce fractions 1-6. Fractions 3-5 were active. Fractions 4 and 5 were further chromatographed on Sephadex LH-20, using gradient elution (100% CH<sub>2</sub>Cl<sub>2</sub>-95% CH<sub>2</sub>Cl<sub>2</sub>/MeOH), to give fractions 4.1-5 and 5.1-3. Fraction 4.2 was again subjected to gradient elution on Sephadex LH-20 to give fractions 4.2.1-3. Fraction 4.2.2 produced guttiferone A (5 mg). Fraction 5.2 was chromatographed on RP C-18 using aqueous MeOH gradient elution (60%-100%) to give fractions 5.2.1-6. Fraction 5.2.5 produced guttiferone G (2.9 mg). Fraction 5.2.2 was chromatographed on Sephadex LH-20, as above, to give fractions 5.2.2.1 and 2. Fraction 5.2.2.1 produced guttiferone A (1 mg).

The hexane fraction was dissolved in EtOAc to give a soluble fraction and an insoluble fraction. The insoluble fraction was recrystallized from CH<sub>2</sub>Cl<sub>2</sub> and MeOH to give friedelin (11.6 mg).

**Guttiferone A (2.6):** yellow oil;  $[\alpha]_D^{+32}$  (*c* 0.04, CHCl<sub>3</sub>); UV (MeOH)  $\lambda_{\max}$  (log  $\epsilon$ ) 233(sh), 258 (4.01), 278 (4.04), 303 (sh), 355 (3.80) nm; <sup>1</sup>H NMR, see Table 2.1; <sup>13</sup>C NMR, see Table 2.1; FABMS *m/z* 601 [M-H]<sup>-</sup> (100), 533 (80), 465 (4), 449 (4), 395 (12), 341 (12), 326 (9), 231 (33).

**Guttiferone G (2.8):** Yellow amorphous solid;  $[\alpha]_D -25^\circ$  (*c* 0.04, CHCl<sub>3</sub>); UV (MeOH)  $\lambda_{\max}$  (log  $\epsilon$ ) 237 (3.96), 278 (3.91), 322 (sh), 360 (sh) nm; IR (film)  $\nu_{\max}$  3382, 2864, 2923, 2854, 1727, 1647, 1600, 1442, 1378, 1290, 1118 cm<sup>-1</sup>; <sup>1</sup>H NMR, see Table 2.9; <sup>13</sup>C NMR, see Table 2.9; FABMS *m/z* 669 [M-H]<sup>-</sup> (100), 601 (16), 533 (35), 464 (3), 395 (6), 341 (6), 325 (5); HRFABMS *m/z* 671.4332 [M+H]<sup>+</sup> (calcd for C<sub>43</sub>H<sub>59</sub>O<sub>6</sub>, 671.4312).

**Friedelin (2.9):** Colorless needles; Mp 256-260°C (lit.<sup>22</sup> 258-260°C);  $[\alpha]_D -27^\circ$  (*c* 0.2, CHCl<sub>3</sub>) <sup>1</sup>H NMR, see Table 2.10; <sup>13</sup>C NMR, see Table 2.10; HRFABMS *m/z* 427.3931 [M+H]<sup>+</sup> (calcd for C<sub>30</sub>H<sub>51</sub>O, 427.3940).

---

<sup>22</sup> Nozaki, H.; Suzuki, H.; Hirayama, T.; Kasai, R.; Wu, R.-Y.; Lee, K.-H. Antitumour Triterpenes of *Maytenus diversifolia*. *Phytochemistry*. **1986**, 25, 479-485.